Hypersonic Inlet Performance from Direct Force Measurements

PAUL H. KUTSCHENREUTER JR.*
General Electric Company, Cincinnati, Ohio

AND

RICHARD L. BALENT†
Air Force Systems Command, Wright Patterson Air Force Base, Ohio

The problem of establishing one-dimensional values of supersonic combustion inlet performance is approached from the standpoint of direct internal drag measurements. Analytically, one-dimensional inlet component efficiencies can be obtained consistent with mass, momentum, and energy considerations as a function of inlet internal drag. Such efficiency values reflect combined shock wave and viscous losses. Direct measurements of model internal drag were made in a hypersonic shock tunnel to determine the experimental feasibility of this concept for an axisymmetric inlet designed for unity mass flow ratio. With this model, effective internal drag isolation was accomplished by physical separation of the model internal surfaces from adjacent parts of the inlet. With such a technique, a correction must be made to the measured internal drag to account for balance cavity forces. The results of this experiment indicate that, through careful model design, the magnitude of such corrections can be minimized and applied to the measured internal force in an accurate and consistent manner.

Nomenclature

A = flow area, ft²
A_c = inlet capture area, ft²
C_{D_i} = internal drag coefficient
D_i = internal drag, lb
c_p = specific heat at constant pressure, ft²/sec²-°R
C_T = net thrust coefficient
F_N = net thrust, lb
F_2 = impulse function, lb
H_2 = total enthalpy, lb-ft/sec
K_1 = influence coefficient
K_2 = mass-momentum-energy parameter
$\dot{m}$ = mass flow, slugs/sec
M = Mach number
N = boundary-layer profile exponent
P = static pressure, lb/ft²
Q_L = heat loss, (ft/sec)²
T = static temperature, °R
u = local velocity for nonuniform flow, fps
V = velocity for uniform or reference flow, fps
y = duct passage height, ft
Z = $\rho_2 V_2^2 y_2(1 - \theta/y_2 - \delta^*/y_2)$, lb
Δ = finite incremental difference notation
Δ^* = mass flow deficiency parameter
δ = boundary-layer thickness, ft
δ^* = boundary-layer displacement thickness, ft
η_R = inlet pressure recovery defined as the ratio of the actual static pressure rise at the diffuser exit enthalpy to the isentropic static pressure rise from freestream conditions to the same diffuser exit enthalpy
θ = boundary-layer momentum thickness, ft
ρ = density ∽ slugs/ft³
ϕ = momentum deficiency parameter

Subscripts

0, 1 = freestream conditions
2 = diffuser exit conditions
1-D = one-dimensional
MOA = momentum-weighted average
MW = mass-weighted average

Introduction

THE performance potential of the supersonic burning ramjet has been widely established on the basis of one-dimensional cycle analyses employing parametric variations of component efficiency parameters.[1, 2] On the basis of these encouraging calculations, experimental programs have been subsequently initiated for the purpose of validating and improving the assumptions of component efficiency proposed for various demonstration vehicle concepts which employ this promising mode of hypersonic air-breathing propulsion. A problem arises, however, in the interpretation of small-scale component test results to substantiate computations of one-dimensional cycle performance when the experimental flow profiles are not uniform and one-dimensional.

The inconsistencies associated with the conversion of nonuniform flow profiles to equivalent one-dimensional profiles have been considered before.[3, 4] When such conversion techniques must be employed in the analysis of a supersonic burning ramjet they take on increased significance and should therefore be re-examined. In regard to inlet performance, the consequences of such averaging techniques are by contrast less pronounced for the subsonic burning ramjet. For the latter case, the nonuniform supersonic flow profiles upstream of the inlet throat are afforded an opportunity to mix to a more uniform flow in the subsonic diffuser. In addition, the increase in flow area of the subsonic diffuser permits the attainment of relatively low values of boundary-layer thickness to duct passage height ratio as compared to supersonic conditions upstream of the inlet throat. In addition, because of the relatively low subsonic exit Mach number, the velocity

Presented as Preprint 64-540 at the AIAA Aerospace Propulsion Meeting, Cleveland, Ohio, May 4–6, 1964; revision received November 4, 1964. This research was conducted by and sponsored by the Air Force Flight Dynamics Laboratory, Research and Technology Division, Air Force Systems Command, Wright Patterson Air Force Base, Ohio.

* Manager, Hypersonic Inlets and Nozzles, Applied Research and Design Operation, Advanced Engine Technology Department. Member AIAA.

† Technical Manager, Internal Aerodynamics, Air Force Flight Dynamics Laboratory, Research and Technology Division. Member AIAA.

difference across the boundary layer is significantly reduced. In comparison, for supersonic burning ramjet inlets, the exit flow profile is not afforded this mixing opportunity; it may be further distorted due to a fixed geometry design constraint, and the ratio of boundary-layer thickness to duct passage height might be relatively large. It is apparent then that use must be made of some appropriate averaging technique to one-dimensionalize experimental data on inlet component performance for use in one-dimensional propulsion system cycle calculations.

Assuming then that a requirement exists for one-dimensionalizing nonuniform flow properties to establish values of component efficiency, a criterion must be established to determine the adequacy of the averaging technique employed. It is proposed that this criterion be the degree of representation of the actual change in the internal total momentum of all the inlet airflow during the compression process. An averaging or one-dimensionalizing process satisfying this criterion would then reflect both shock losses as well as viscous losses, and by definition would permit correct representation of the inlet internal drag and burner entrance flow momentum when used in one-dimensional propulsion system cycle calculations. In this article, different averaging techniques are evaluated against this criterion. The concept of "drag equivalent" pressure recovery which is consistent with it is discussed in detail. Results of an experimental program establishing the feasibility of determining the "drag equivalent" pressure recovery from direct force measurements are presented.

Core Flow Efficiency

Perhaps the simplest averaging technique is that involving only the consideration of the values of fluid properties contained in the "core flow." When the nonuniform exit flow profile is composed of a one-dimensional core consisting of uniform flow properties plus a nonuniform component of boundary-layer flow (Fig. 1), it can be argued in many cases that there is by comparison with the core flow, much less mass flow in the boundary layer. Thus core flow efficiencies may be representative of the complete process efficiency. This technique has much appeal, because core flow performance is by comparison much easier to obtain experimentally than other methods that require essentially complete flow profile measurement. The argument against this concept even at the conditions previously described is illustrated by the curves of Fig. 2.

These curves were generated at the selected combinations of M_0, A_1/A_2, and core flow η_R assuming the existence of a laminar boundary layer represented by the profile parameter $N = 1$ at station 2. For such core flow conditions, there are many solutions for the actual C_{Di}, each being determined by the particular value of δ^*/y_2 consistent with the continuity equation

$$\frac{\delta^*}{y_2} = 1 - \frac{y_1}{y_2}\left(\frac{T_1}{T_2}\right)^3 \frac{M_0}{M_2}\frac{1}{\eta_R} \tag{1}$$

and the momentum equation

$$C_{Di} = 2\left[1 - \frac{q_2}{q_1}\frac{y_2}{y_1}\left\{1 - \frac{\delta}{y_2}\left(\frac{\delta^*}{\delta} + \frac{\theta}{\delta}\right)\right\}\right] - \left[\frac{y_2}{y_1}\frac{P_1}{q_1}\left(\frac{P_2}{P_1} - 1\right)\right] \tag{2}$$

The numerical results indicate the degree to which the actual change in total momentum of the inlet airflow, i.e., the inlet internal drag, can be underestimated when core flow efficiency values are used.

For those cases where this deviation is significant, two alternative approaches immediately suggest themselves. The first is that of using an effective area ratio in conjunction with the core flow efficiency. With this approach, however,

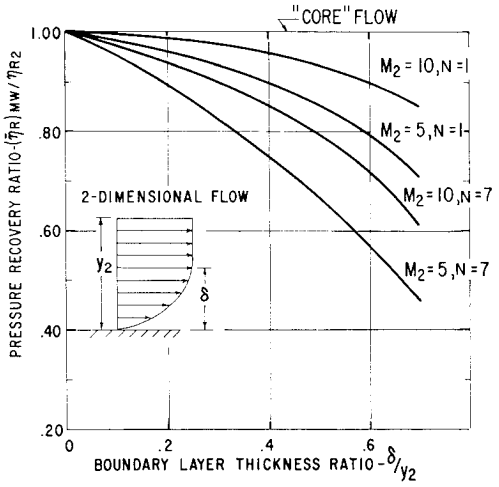

Fig. 1 Comparison of core flow and mass weighted η_R.

the experimental attractiveness of the core flow concept degenerates somewhat because now there is a requirement to provide enough additional instrumentation to determine the appropriate effective area ratio. Except for those cases of constant static pressure across the entire duct exit area, the instrumentation requirements rapidly approach those for complete profile measurement. In addition, knowledge or estimates of this effective area ratio (an additional variable) are required for all conditions at which the propulsion system performance is to be calculated. The second alternative is that of seeking an average value of one-dimensional component efficiency based on the complete nonuniform profile shape. Several approaches to this alternative are considered in the next section.

Mass and Momentum Averages

When seeking an average fluid property value for a nonuniform flow profile, the concept of averaging with respect to mass flow or momentum is relatively common practice.

As defined here

$$\bar{x}_{MW} \equiv \frac{1}{\rho_0 V_0 A}\int_{A_2} \rho x u dA \tag{3}$$

$$\bar{x}_{MOA} \equiv \frac{1}{z}\int_{A_2} \rho x u^2 dA \tag{4}$$

and applied to a nonuniform flow with a finite uniform one-dimensional core (Fig. 1), it can be shown for the case of con-

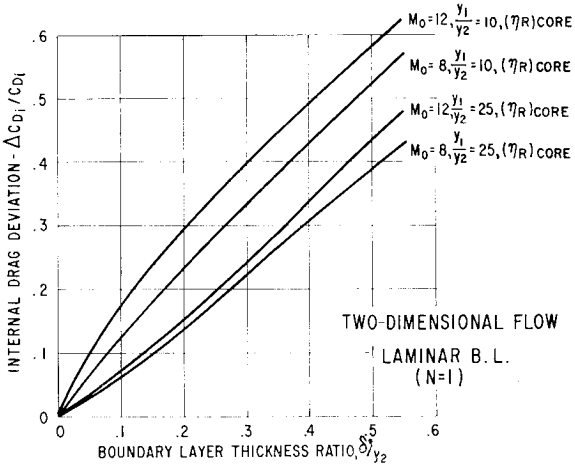

Fig. 2 Effect of core flow averaging on C_{Di}.

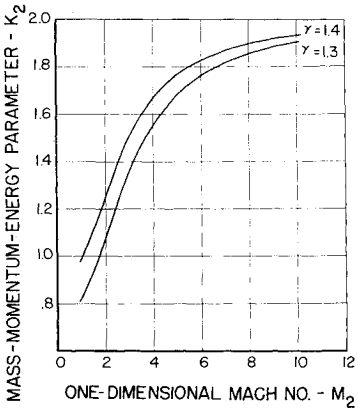

Fig. 3 Mass-momentum-energy parameter K_2.

stant static pressure across the duct that $\bar{x}_{MW}$ is slightly less than $\bar{x}_{MOA}$.

Applying the more conservative mass averaging technique to the component efficiency parameter inlet pressure recovery, the results of Fig. 1 indicate that significant numerical deviations from the core flow value occur only for large values of boundary-layer thickness to duct passage height. At conditions of relatively low boundary-layer thickness ratio, it is to be expected that utilization of mass and momentum averaging would give results similar to those obtained from direct use of core flow values alone. Relatively large values of boundary-layer thickness ratio are not uncommon in small scale inlet tests conducted in current ground test facilities, however. As will be shown in a later section, use of the mass-weighted pressure recovery does, of course, result in an improvement over the use of core flow values alone, but it can still lead to significant underestimation of the internal drag. Here again, the situation could be improved with the use of an effective exit flow area rather than the geometrical area. Since this could presumably be determined without instrumentation beyond that already required to accurately determine the flow profile shape, it represents no apparent additional experimental difficulty.

Drag Equivalent Pressure Recovery

If instrumentation sufficient for accurately determining the flow profile shape can be provided, a further improvement can be realized; an ideally exact representation of the inlet internal drag or burner entrance flow momentum can be achieved. From integration of such profile data,

$$F_2 = \int_{A_2} P(\gamma M^2 + 1)dA \equiv [PA(\gamma M^2 + 1)]_{1-D} \quad (5)$$

$$\dot{m}_2 = \int_{A_2} \rho u dA \equiv \left[\frac{\gamma PAM^2}{V}\right]_{1-D} \quad (6)$$

$$H_2 = \int_{A_2} \left(\rho u c_p T + \frac{\rho u^3}{2}\right)dA \equiv$$

$$\left[PAV\left(\frac{\gamma}{\gamma - 1} + \frac{\gamma M^2}{2}\right)\right]_{1-D} \quad (7)$$

from which the quantity

$$K_2 \equiv \frac{(F_2)^2}{\dot{m}_2 H_2} = \frac{(\gamma M_2^2 + 1)^2}{(\gamma M_2)^2\,([1/(\gamma - 1)] + (M_2^2/2))} \quad (8)$$

is seen to be a function only of the one-dimensional Mach number M_2. This function K_2 is plotted in Fig. 3 for $\gamma = 1.3$ and 1.4. Thus from integration of the nonuniform flow profile shape, a one-dimensional Mach number M_2 can be determined which simultaneously satisfies the equations of conservation of mass, momentum, and energy. It is significant to note that such an M_2 is independent of A_2 or P_2, but choice of one determines the value of the other. For instance, if A_2 is assumed to be the physical flow area, the result is actually a constant-area mixing solution, and a one-dimensional value of P_2 less than actual can result. The corresponding one-dimensional value of inlet pressure recovery would necessarily be the lowest possible value for a one-dimensional solution. On the other hand, choice of a one-dimensional static pressure equal to some greater measured value results in a constant-pressure mixing solution with an effective flow area less than the physical flow area. Correspondingly, the pressure recovery value for the constant-pressure mixing solution would be greater than the value obtained from the constant-area mixing solution.

The foregoing is the basis for what has been designated as the "drag equivalent" pressure recovery. Such a one-dimensional value, by its very formulation, must satisfy the criteria set forth in the Introduction. Its accurate evaluation from flow profile measurements may pose a rather difficult physical problem for small-scale hypersonic inlets with even moderately high contraction, however. Consideration of probe interference, cooling, and lag time limit the number of pitot probes that can be employed. For high-temperature flow with cooled walls, measurements of the variation in the total temperature profile may be required. For fixed-geometry inlets, flow profile distortion at least at off-design Mach numbers may introduce the additional requirement for surveys of static pressure variation across the duct.

In approaching the question of anticipated levels of accuracy in establishing integrated flow properties from profile measurements, simple calculations using power-law-type profiles show that the order of 8 to 10 probes per half-passage-height are generally required to maintain reasonable levels of accuracy in determining F_2. For nonideal application where the profile shape is more irregular and the static pressure may vary across the duct, it is to be expected that an additional number of probes would be required to maintain comparable accuracy levels.

The importance of discrepancies in inlet performance representation on over-all supersonic combustion ramjet performance is difficult to accurately assess in a generalized manner. Specific engine geometry as well as inlet, burner, and nozzle thermodynamics can play an important role. A discrepancy in the one-dimensional representation of inlet pressure recovery represents a direct discrepancy in the representation of inlet internal drag and thus in burner entrance flow impulse F_2. However, with the aid of the following approximation

$$\Delta D_i/F_N \approx -[(2 - C_{Di})/C_T]\cdot(\Delta F_2/F_2) \quad (9)$$

changes in inlet internal drag brought about by discrepancies in F_2 can be viewed in terms of engine net thrust fraction. As written, consideration is not given to the fact that one-dimensionally the engine choking equivalence ratio and other thermodynamic phenomena are influenced by the value of F_2 used in the cycle analysis. The latter effects on the reference net thrust may tend to offset the effects of such changes in F_2

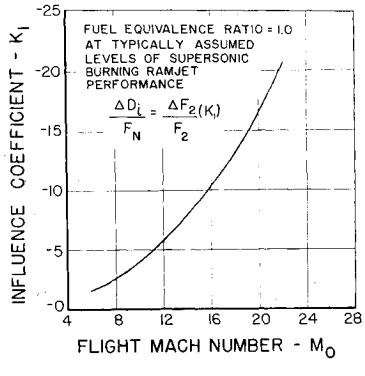

Fig. 4 Influence coefficient K_I vs flight Mach number.

at some flight conditions. The value of such a comparison is that, should small drag fractions be indicated, the implication would be that one could afford to be less concerned about this aspect of one-dimensional inlet performance representation.

On this basis, the preceding equation was evaluated for typically quoted levels of supersonic combustion ramjet performance and inlet geometry. Although use of different engine geometry and other levels of component efficiency will alter the values shown in Fig. 4, the indicated need for greater accuracy with increasing flight Mach number is quite pronounced.

Direct Force Measurement Approach

Although the study of exit flow profiles are necessary for obtaining a better understanding of the inlet compression process, it appears in light of the previous discussions that, when the primary test objectives are the establishment of appropriate one-dimensional values of inlet component efficiency, then direct force measurements[5] may be quite adequate. Such an approach can result in direct determination of inlet internal drag and one-dimensional burner entrance momentum. In those cases where flow profile distortion makes accurate interpretation of flow profile data difficult, direct measurements of model internal drag may be even more desirable.

On this basis, it is convenient to rewrite the equations of conservation of mass, momentum, and energy as follows:

Continuity

$$\rho_2 V_2 A_2 = \rho_0 V_0 A_0 \tag{10}$$

Momentum

$$D_i = \dot{m} V_0 + D_A - \dot{m} V_2 - A_2(P_2 - P_0) \tag{11}$$

Energy

$$c_P T_0 + (V_0^2/2) = c_P T_2 + (V_2^2/2) + Q_L \tag{12}$$

Examination of the equations in this form indicate that in order to establish F_2 and other computed flow properties from direct force measurement, it is necessary to know not only the inlet mass flow ratio but also the inlet additive drag. In addition, it is to be noted that such formulation does not directly account for the effect of nonaxial velocity components. The latter is not considered to be critical in that such nonaxial components must necessarily be small in high performance inlets designed for use with axially aligned burners.

Using equations similar to those given previously, the calculation procedure for establishing the one-dimensional drag equivalent pressure recovery is presented in detail for the case of nonadiabatic flow of a reacting thermally perfect gas in equilibrium in Appendix I of Ref. 6. For most ground testing of small-scale inlets, however, the temperatures are usually low enough that dissociation effects can be neglected and only caloric imperfections considered. For the case of unity mass flow ratio, at given freestream conditions Q_L and A_1/A_2, the internal drag coefficient can be expressed as a function of the single variable T_2. Choice of a range of T_2 then permits the determination of curves of η_R vs C_{D_i} as presented in Fig. 5.

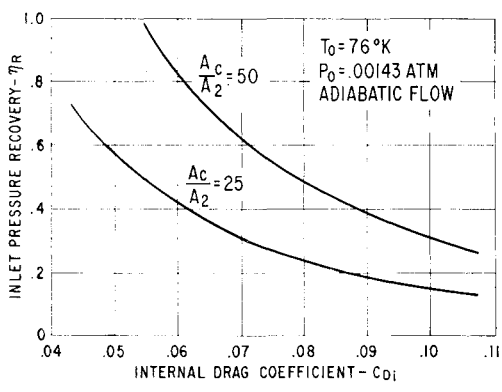

Fig. 5 Mach 16 parametric inlet performance.

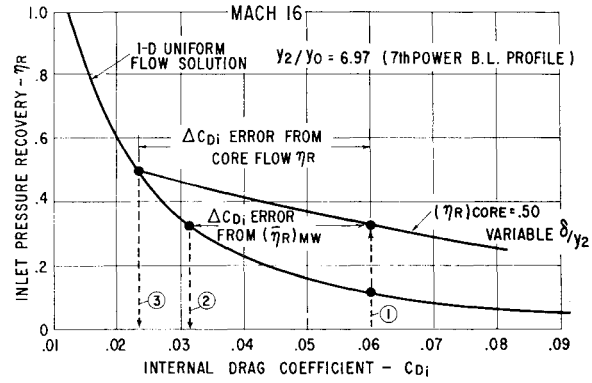

Fig. 6 Effect on C_{D_i} of one-dimensional weighting of η_R.

With the aid of such curves, a relative comparison of the use of the drag-equivalent, mass-weighted, and core-flow pressure recoveries can be made. Such a comparison is presented in Fig. 6. At condition 1, integration of the exit flow profile establishes the actual value of internal drag coefficient and the intercept with the one-dimensional uniform flow solution curve of η_R vs C_{D_i} defines the drag equivalent pressure recovery. The exit flow profile for this particular example had a core flow pressure recovery of 50%. The line of $(\eta_R)_{core} = 0.50$ represents the mass weighted pressure recovery for a family of seventh power velocity profiles with variable δ/y and constant value of core flow pressure recovery. At the actual value of C_{D_i} (condition 1), use of the mass flow weighted value of η_R infers the value of C_{D_i} indicated at 2, and use of the core flow η_R infers the value of C_{D_i} indicated at 3. The deviation of the inferred values of C_{D_i} from the actual value at 1 is thus obtained for identical exit flow profiles as a function of the one-dimensionalizing technique employed.

This deviation from the actual internal drag inferred by the use of either core flow or mass weighted values of η_R in conjunction with the inlet geometrical area ratio has been found to be most pronounced for high performance inlets with relatively low contraction ratio, and of minimum variation for low performance inlets with high contraction ratio. Since the one-dimensional value of inlet component efficiency, drag-equivalent pressure recovery, must permit exact representation of the change in internal total momentum of the inlet airflow for all cases, it seems in this sense to be ideally suited for use in one-dimensional cycle calculations.

Uniform Flow Parametric Calculations

Presented in this section are results obtained from simultaneous solution of Eqs. (10–12) for the case of unity inlet mass flow ratio. As presented, these results also represent the uniform flow constant area mixing solution for a nonuniform exit flow with the same integrated value of F_2 as the one-dimensional value. This would correspond to the same integrated value of internal drag C_{D_i} as the one-dimensional value. Thus direct measurement of C_{D_i} would in turn permit determination of required one-dimensional flow properties.

In Fig. 7, the curves of η_R vs C_{D_i} are bounded at one end by conditions of 100% pressure recovery, and at the other end by one-dimensional choking. As pointed out in Ref. 6, lines of inlet static enthalpy ratio superimposed on such curves are almost vertical for hypersonic freestream conditions, independent of inlet contraction ratio. In Fig. 8, the static pressure ratio solution is presented for the curves of Fig. 7. In Figs. 9 and 10, the effect of heat loss can be noted. As would be expected, this effect is most pronounced when the amount

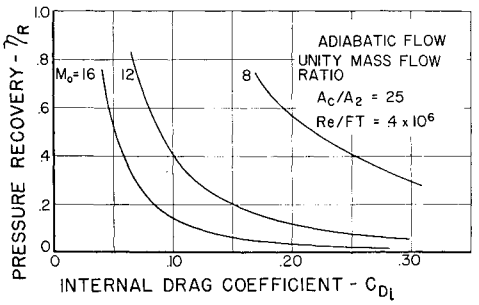

Fig. 7 Cosntant-area mixing solution for η_R vs C_{Di}.

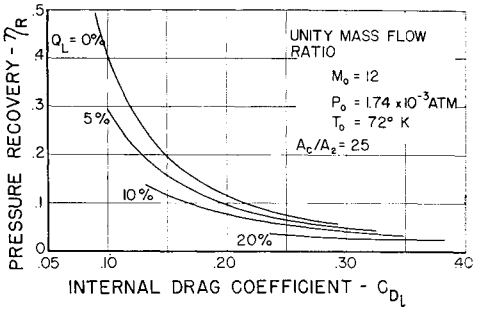

Fig. 9 Parametric effect of heat loss on η_R.

of heat transferred is of the order of the inlet static enthalpy rise.

Nonuniform Flow Formulation and Parametric Results

To provide a basis for obtaining the constant-pressure mixing solution, the continuity and momentum equations can be rewritten in familiar integral parameter notation

$$\rho_0 V_0 A_0 = \rho_2 V_2 (A_2 - \delta^*) \tag{13}$$

$$D_i = \dot{m} V_0 + D_A - A_2(P_2 - P_0) - \rho_2 V_2^2 (A_2 - \theta - \delta^*) \tag{14}$$

For ducts with irregular cross-sectional shape where the local displacement thickness δ^* may not be concentrically uniform around the circumference, it is convenient to replace δ^* and θ in the preceding equations with the following defined parameters:

$$\Delta^* \equiv \int_{A_2} \left(1 - \frac{\rho u}{\rho_2 V_2}\right) dA \qquad \phi \equiv \int_{A_2} \left(1 - \frac{u}{V_2}\right) \frac{\rho u}{\rho_2 V_2} dA$$

Although evaluation of such parameters would ordinarily require flow profile instrumentation, an approximation is possible simply by adding duct-exit static pressure instrumentation to a force model. Such an approach requires, however, that $\phi \ll \Delta^*$, which, by analogy with θ and δ^* at hypersonic speeds, would appear to be a reasonable assumption to a first approximation. Following such a procedure, having established both the model internal drag and exit static pressure level, the corresponding Δ^*/A_2 can be determined as indicated in Fig. 11 and the one-dimensional constant pressure solution drag equivalent pressure recovery established as in Fig. 12.

Force Model Design

Aerodynamic

The previous sections indicated the manner in which the drag-equivalent pressure recovery could be established assuming the required drag measurements could be made. A hypersonic inlet model was specifically designed[7] to determine whether the required drag measurements could be obtained from direct force measurements in a hypersonic shock tunnel. Although this model was specifically tailored for this purpose, consideration was also given to the simulation of particular full-scale supersonic-burning-ramjet inlet design characteristics. A requirement was also established that the configuration selected should be reasonably amenable to theoretical analysis in order to provide the additional opportunity of checking the adequacy of existing inlet performance estimation techniques.

The inlet configuration selected for this investigation was an axisymmetric, external-internal compression design with an "X" shock-wave system supported by intermediate isentropic compression. For the scheduled test Mach numbers, the inlet was designed to operate at unity mass flow ratio. A design point Mach number of 16.0 was selected at a unit Reynolds number of 10^5 based on anticipated test conditions in the Cornell Aeronautical Laboratory 48-in. shock tunnel.[8] Design point calculations at these operating conditions were made assuming that the boundary layer was laminar and attached. The inlet wall contours were corrected for the laminar boundary-layer growth by means of an iterative combination method of characteristics solution[9] of the "effective" body comprised of the actual wall contour and the laminar boundary-layer displacement thickness.[10] The actual wall contour was continually modified until the iterated "effective" body had the desired characteristics solution for the inviscid flow. A photograph of the fabricated model is shown in Fig. 13. (The steep external cowl angle is required for balance installation.)

Experimental considerations dictated that the internal duct contours be designed so that positive drag loads always act on both the centerbody and the cowl. Otherwise, accurate measurement of small component forces becomes a difficult problem for a balance system that must be capable of accurately measuring much larger loads at other test conditions. For this reason, the internal duct lines were designed to achieve stream-aligned flow at the exit. A cross-section of the model internal lines is presented in the drawing of Fig. 14.

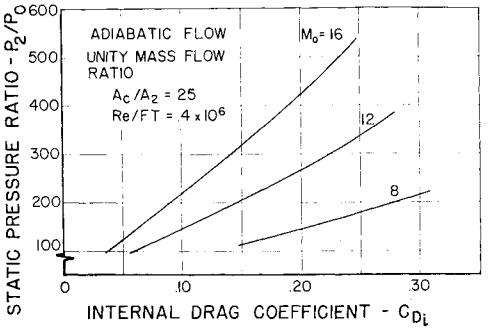

Fig. 8 Constant-area mixing solution for P_2/P_0 vs C_{Di}.

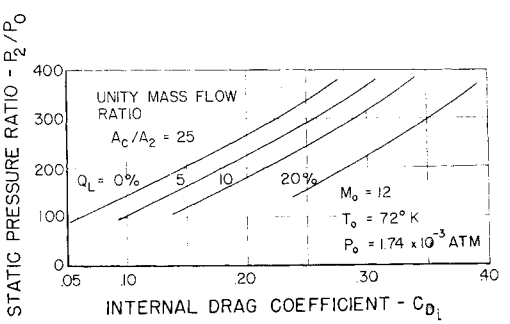

Fig. 10 Parametric effect of heat loss on P_2/P_0.

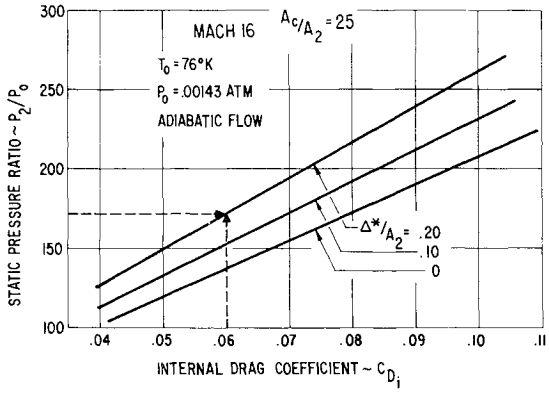

Fig. 11 Constant-pressure mixing solution for P_2/P_0 vs C_{Di}.

To provide experimental flexibility, provision was made for fore and aft spike translation but at a constant value of inlet geometric contraction ratio. The aft portion (nonmetric) of the constant-area duct and the high adverse pressure gradient region of the centerbody were instrumented with static pressure transducers to provide direct indication of the degree of actual compression achieved and to provide an indication of the static pressure variation along and across the constant-area duct. Thin-film heat-transfer gages were installed in the high adverse pressure gradient region of the centerbody, and, for several runs, pitot tubes were added at the exit of the constant area throat region.

Aeromechanical

The translation of the aerodynamic model lines into actual test hardware was the result of a joint effort with the Cornell Aeronautical Laboratory under Air Force Contract AF33(657)-11414, which also provided for model testing. Although force balance drag measurements for external aerodynamic models are quite common, such models do not generally require the same degree of actual mechanical drag isolation. The complete inlet drag (both external and internal) could be measured; however, some method of subtracting the external drag has to be devised if the values of drag-equivalent pressure recovery are to have any reasonable resemblence to the actual quantities at the exit station of the diffuser.

The required drag isolation is accomplished by the use of metric and nonmetric surfaces. These surfaces are physically isolated from each other, and separate balances are used to measure the forces on the metric cowl and the metric spike surfaces. This arrangement is evident in Fig. 14. The gap distance between the metric and nonmetric surfaces is approximately 0.020 in. wide. Calculations indicated that less than 1% of the inlet mass flow would bleed through these gaps in the constant-area "throat" section. Because of the relatively low volume of the balance cavity, transient calculations indicated that significant increases in cavity pressure (above tunnel ambient) would occur even during the few milliseconds of steady-state inlet operation. To limit the resulting "thrust" forces on the gap rim in the constant-area duct to a small fraction of the measured internal drag, provisions were made for venting the balance cavity and beveling the gap rim as indicated in Fig. 14.

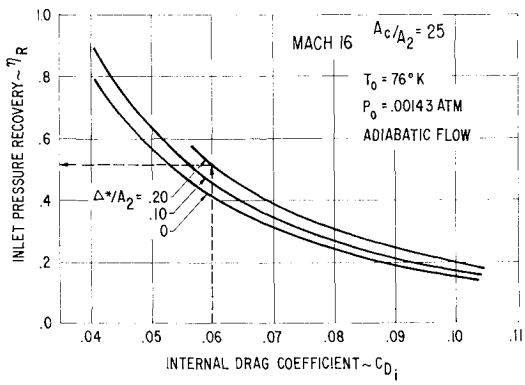

Fig. 12 Constant-pressure mixing solution for η_R vs C_{Di}.

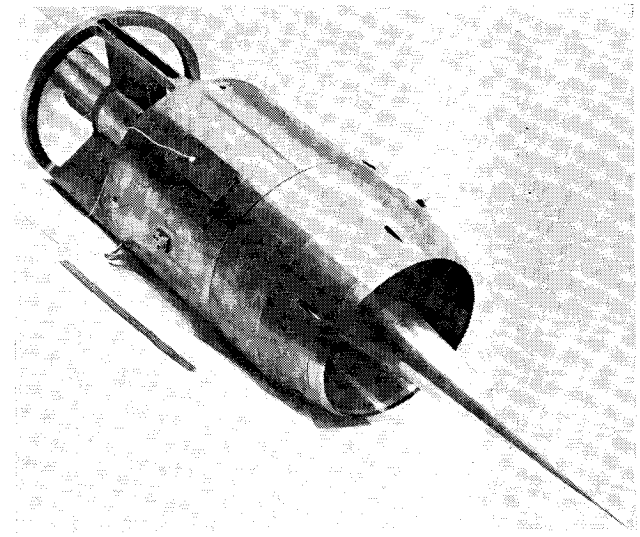

Fig. 13 Axisymmetric inlet force model.

Mass flow into the inner balance cavity was minimized through the use of labyrinth seals at both the upstream and downstream edges of the metric surfaces. On the cowl, this amounts to omission of the leading edge drag increment (a relatively small correction for sharp leading edges, and one that can be made analytically with a reasonable degree of certainty). Cowl-lip-bluntness drag could have been included in the direct force measurement by locating the labyrinth seals externally on the cowl instead of internally. Such an external location, because of the higher local static pressure, represents a more critical sealing problem and could result in larger corrections to the measured internal force to compensate for balance cavity pressure effects. For these reasons, the cowl leading edge seal was located internally, and an analytical correction was made to account for lip bluntness drag. With the inlet configuration of Fig. 13, this correction amounts to less than 4% of the measured internal drag at Mach 12.

Experimental Results

Two series of force tests consisting of 40 shots were performed in the Cornell Aeronautical Laboratory 48-in. shock tunnel at Mach numbers of 8, 12, 14, and 16 with a systematic variation in unit Reynolds number at each Mach number.

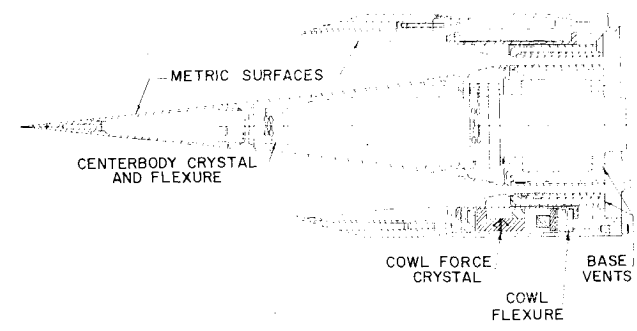

Fig. 14 Cross-section schematic of inlet force model.

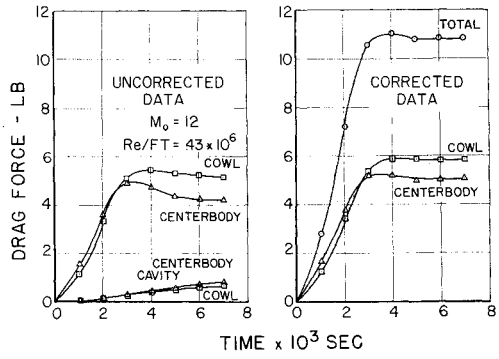

Fig. 15 Typical force data with attached boundary layer.

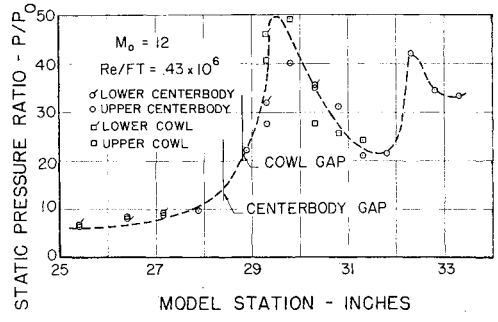

Fig. 17 Typical static pressure data with attached boundary layer.

Other test variables included spike bluntness and a small amount of centerbody travel. Schlieren movies were taken at the majority of the test conditions. The major difference between the two series of tests was the addition of static pressure transducers and thin-film heat-transfer gages in the high adverse pressure gradient region (metric surface) of the centerbody. Three pitot probes aft of the constant-area throat region were also provided in the second test phase. This instrumentation was added in an attempt to determine the intersection of the cowl shock on the centerbody and also to obtain core flow total pressure recovery measurements.

A typical Mach 12 force trace is replotted in Fig. 15 for $Re/\text{ft} = 0.43 \times 10^6$. The cowl and centerbody curves have been taken directly from the force data traces. The centerbody cavity and cowl cavity plots have been obtained from calculations based on metric surface projected area and internal cavity pressure measurements. For this rather large model (10-in. capture diameter), steady-state force measurements were obtained after approximately 3 to 4 msec, measured from the initiation of tunnel starting. After 4 msec, correction of the measured force data, by addition of the computed cavity force, results in an essentially flat curve for total internal drag as well as a flat component drag history. Although the cavity pressure correction represents a larger fraction of the measured internal drag than originally anticipated, judging from the flatness of the corrected data, it is a correction that can be made quite consistently and accurately.

At some test conditions, inlet boundary-layer separation was detected. It is interesting to note that in some of these cases although the separation propagated upstream on the inlet spike, past the cowl, lip station, steady-state inlet operation was achieved, and the inlet remained started at full mass flow ratio. Such separation was clearly evident in the schlieren movies and was further substantiated by observation of static pressure, heat flux, and force data time histories.

Although no such evidence of boundary-layer separation was found to exist in the data of Fig. 15, a reduction in free-stream unit Reynolds number (Re/ft) to 0.1×10^6 caused the inlet boundary layer to separate. This low-Reynolds-number, separated-flow force data is presented in Fig. 16. Although again approximately 4 msec were required for a peak force measurement, the data indicate an additional 2 msec were required to obtain steady-state force readings with a stabilized separated boundary layer. The static pressure data at this condition indicate throat static pressure ratios (P/P_0) two to three times greater than those measured when no boundary-layer separation was observed. Comparison of the maximum steady-state drag levels as indicated by Figs. 15 and 16 suggest that, even though the pressure drag of the metric surface may have risen sharply as a result of the boundary-layer separation, this was more than compensated for by reductions in local skin-friction drag.

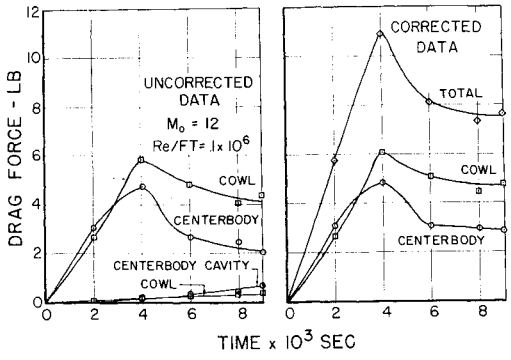

Fig. 16 Typical force data with boundary-layer separation.

The extent of the separated boundary layer at $M_0 = 16$ and $Re/\text{ft} = 0.1 \times 10^6$ was severe enough to cause the inlet to unstart. This unstart problem at Mach 16 was later eliminated by increasing Re, but the separation problem remained.

Typical static pressure data are presented in Fig. 17 for the test conditions of Fig. 15. The constant-area throat begins on the metric surfaces approximately 0.20 in. upstream of the 0.020-in. gap between the metric and nonmetric surfaces. Considering the latter, it can be seen from the data of Fig. 17 that the pressure rise from the impinging cowl and centerbody shock waves extended downstream of the centerbody and cowl shoulders, well into the constant-area duct. In spite of such rapidly changing flow characteristics, it is interesting to note that a relatively high degree of flow symmetry was achieved as recorded by the upper and lower surface pressure transducers. The static pressure deviation between the cowl and centerbody resulted in the use of a numerical average pressure rise ratio for data reduction purposes such as required for estimation of Δ^*/A_2.

The inlet pitot pressure was recorded in the second series of tests by adding three probes to the exit of the constant-area throat region. These probes were located 120° apart, and since they were in the center of the passage height, they served only to give an indication of the core flow total pressure recovery. As would be expected, these readings were considerably higher than the drag derived pressure recovery values. Complete inlet performance details, which are considered classified, will be included in a final report currently being prepared by the Air Force Flight Dynamics Laboratory.

Concluding Remarks

The method of establishing over-all inlet performance from direct force measurements is well suited for the determination of one-dimensional inlet efficiency such as that required for cycle analysis of supersonic combustion ramjets. Such a technique can result in the accurate representation of combined viscous and shock losses. The experimental feasibility of this technique depends to a great extent on the isolation of the internal and external drag forces as well as knowledge of inlet airflow and additive drag. In the described

experiment, the latter problem was eliminated since the inlet was designed for unity mass flow ratio. Effective internal drag isolation was accomplished with an axisymmetric inlet through the use of metric and nonmetric surfaces. With such a technique, it was found that the associated corrections to the measured drag levels to account for lip bluntness drag and balance cavity internal forces could be made both accurately and consistently. Careful model design can also minimize the magnitude of such corrections. It is to be expected, however, that comparable degrees of internal drag isolation and performance will be more difficult to achieve with three-dimensional inlet designs.

References

[1] Molder, S., "Cruise and boost performance of hypersonic ramjets," McGill Univ., Montreal, Canada, Mechanical Engineering Dept. Rept. TN62-3 (1962).

[2] Marino, A. and Mandel, H., "Performance of the hypersonic ramjet with hydrogen," General Applied Science Labs., TR 198 (October 1960).

[3] McLafferty, G., "Generalized approach to the definition of average flow quantities in non-uniform streams," United Aircraft Corp. Rept. SR 13534-9 (December 1955).

[4] Wyatt, D. D., "Analysis of errors introduced by several methods of weighting non-uniform duct flows," NACA TN3400 (March 1955).

[5] Kutschenreuter, P. H., Jr., "Force balance determination of supersonic/hypersonic combustion inlet performance levels," J. Aerospace Sci. **29**, 1389–1390 (1962).

[6] Kutschenreuter, P. H., Jr., "Force balance determination of inlet performance for advanced vehicle applications to orbital velocities using internal drag measurements," Aeronautical Systems Div., TDR-63-701 (September 1963).

[7] Kutschenreuter, P. H., Jr., Balent, R. L., and Richey, G. K., "Design analysis summary of two force balance hypersonic inlet configurations," Flight Dynamics Lab. TDR-64-19 (March 1964).

[8] "48-inch hypersonic shock tunnel—description and capabilities," Cornell Aeronautical Lab. Rept. (December 1962).

[9] Balent, R. L., "Application of the method of characteristics to various inlet compression surfaces," ASRMM-TM-63-1 (June 1963).

[10] Rickey, G. K., "Applications of compressible lanunar and turbulent boundary layer analysis to the design of inlet compression surfaces," ASRMM-TM-63-2 (June 1963).

MARCH-APRIL 1965 J. SPACECRAFT VOL. 2, NO. 2

Shock-Induced Supersonic Combustion in a Constant-Area Duct

P. M. Rubins* and T. H. M. Cunningham†
ARO, Inc., Arnold Air Force Station, Tenn.

A two-oblique-shock compression was used as a reaction-initiating mechanism for the H_2-air reaction in a constant-area duct while maintaining supersonic flow. Gradual pressure rise from the chemical heat release was observed as the fuel concentration was increased until the duct flow was choked. The aerodynamic, thermodynamic, and chemical kinetic problems are discussed. For the small model used, it was found that the generation of a turbulent boundary layer was necessary to prevent thermally produced pressure rise from causing boundary-layer separation and premature choking. It is concluded that shock-induced combustion 1) is experimentally feasible in ducted flow, 2) can be controlled by varying inlet temperature, pressure, Mach number, or fuel concentration, 3) may be analyzed as a one-dimensional flow for the small models investigated if average stream properties are used, and 4) experimentally produces ignition delay times that agree with existing chemical kinetic flow computations within the accuracy that stream properties can be determined. The possible use of shock-induced combustion for air-breathing hypersonic propulsion is discussed.

Nomenclature

A = area
C_p = specific heat at constant pressure (refers to air when no additional subscripts are used)
D = duct diameter
ER = equivalence ratio
d = ignition delay distance
F = stream force
f = fuel-air ratio
L = duct length
M = Mach number
p = static pressure
p_t = stagnation pressure
p_t' = pitot pressure
Q = heat flux
T = static temperature, °R
T_t = stagnation temperature, °R

Presented as Preprint 64-84 at the AIAA Aerospace Sciences Meeting, New York, January 20–22, 1964; revision received November 4, 1964. The research reported in this paper was sponsored by Arnold Engineering Development Center, Air Force Systems Command, under Contract No. AF 40(600)-1000 with ARO, Inc. Further reproduction is authorized to satisfy needs of the U. S. Government. The authors acknowledge the cooperation of A. A. Westenberg and S. Favin of the Johns Hopkins University, Applied Physics Laboratory for the use of their H_2-air computer program, as well as the previous assistance and use of a similar program developed by P. A. Libby and H. Pergament at General Applied Science Laboratories. We are also indebted to C. E. Peters and R. P. Rhodes Jr. at Arnold Engineering Development Center for helpful suggestions during the course of the work. Anna Parker assisted in the editorial work. This work was supported by the Air Force Office of Aerospace Research through the Arnold Engineering Development Center, Air Force Systems Command.

* Research Project Engineer, Research Branch, Rocket Test Facility. Member AIAA.
† Research Engineer, Research Branch, Rocket Test Facility.